Evaluating and forecasting methods for assessing the health status of cables under the load of large-scale electric vehicle charging

He Lei*, Li Rufeng, Tang Baofeng, Zhou Kaifeng, Jia Binyu and Xue Lin

State Grid XiongAn New Area Electric Power Supply Company, Xiong'an New Area, Hebei, China

The assessment of the health status and prediction of the lifespan of cable equipment are critical for ensuring the stability and efficiency of the power grid. This paper develops a temperature-current-capacity-life calculation model for cables, considering the fast and slow charging demands of electric vehicles (EVs). Analyses under scenarios of rapid and slow charging demands are conducted, introducing a cable health index and establishing a health status assessment framework based on this index. The framework accounts for various factors leading to cable faults, offering a comprehensive evaluation of the health status of cables with different fault rates. Building upon this, a prediction method using the Fire Hawk Optimization (FHO) Algorithm and Convolutional Neural Network (CNN) is proposed. This method enhances performance by optimizing the hyperparameters of Bidirectional Gated Recurrent Unit (BiGRU) through FHO, effectively searching and determining the optimal hyperparameter configuration. The impact of different scenarios and varying EV penetration rates on cable temperature is analyzed through case studies, facilitating the assessment and prediction of health status.

1 Introduction

As modern society's reliance on electricity intensifies, cables, being an indispensable component of the power grid, play a pivotal role in ensuring the safety and reliability of the entire electrical system (Rajendran et al., 2021). The escalating demand for electric vehicle (EV) charging, especially the high current requirements of direct current fast charging, raises challenges for cable equipment, leading to increased cable temperatures (Gupta et al., 2021). This not only impacts their performance and lifespan but also poses potential safety hazards. Moreover, cable equipment is subject to various internal and external factors such as aging, climate change, and operational stress, leading to potential performance deterioration over time (Hossain et al., 2021). Therefore, the health assessment and prediction of cable equipment's status are of paramount importance.

Cables are designed with a lifespan of approximately 40 years, predominantly affected by thermal aging and electrical aging (Li et al., 2007). Thermal aging suggests that a cable's lifespan is mainly influenced by load rate, insulation material properties, and ambient

temperature, whereas electrical aging posits that a cable's expected lifespan is inversely proportional to insulation field strength, as proven in relevant studies. Research documented in (Nemati et al., 2019) utilizes the Weibull parametric proportional hazard model to estimate the failure rate of each cable based on its years of usage and a set of explanatory factors (Dinmohammadi et al., 2019). proposes a lifespan prediction model for submarine cables under specific seabed conditions and tidal flows, predicting the expected lifespan of cables affected by erosion and wear. Further (Montanari et al., 2019), assesses the insulation condition of electrical equipment as a function of operating time, evaluating the feasibility and scope of maintenance measures and life extension plans based on aging and life models (Wang et al., 2019). examines the impact of EV charging loads on the temperature and thermal life of distribution network cables, focusing on the harmonic characteristics of 3.3 kW and 6.6 kW AC slow charging under peak and off-peak scenarios. However, in the context of dual carbon goals, the continuous increase in EV ownership, reaching 18.21 million in China by September 2023, and the establishment of DC fast charging and even Chaoji fast charging standards, allowing charging powers up to an astonishing 900 kW, impose higher current loads on cables (Yu et al., 2022). Excessive current loads can lead to overheating and material degradation, reducing the efficiency and reliability of cables (Li and Li, 2017). Research in this specific area is not yet comprehensive, and the lifespan prediction of operational cables needs to consider stochastic characteristics, including faults due to defects, external damage, and environmental factors.

In the realm of cable equipment health monitoring and lifespan prediction, numerous domestic and international researchers have pioneered a variety of innovative methods, broadly categorized into model-based predictions and data-based predictions (Liao and Kottig, 2014). Model-based predictions focus on in-depth analysis of cable equipment's structure and material properties, often involving complex fault mechanism mathematical models (Ahmad et al., 2022). However, due to their high complexity, the practical application of these methods is somewhat limited. On the other hand, data-based prediction methods do not require an in-depth understanding of mechanisms; instead, they assess the health and predict the lifespan of equipment by analyzing data and measurement parameters collected by sensors. These methods are further divided into statistical methods and machine learning methods (Carvalho et al., 2019). Traditional machine learning methods, such as Support Vector Machine (SVM) (Yan et al., 2020) and Random Forest (RF) (Gan et al., 2022), are favored for their flexibility and efficiency in extracting shallow features for health assessment and lifespan prediction. The latest research trend is employing deep learning technologies, particularly CNN and Recurrent Neural Networks (RNN) (Han et al., 2021), to process cable data, aiming to enhance prediction accuracy and robustness. The application of deep learning in cable equipment's lifespan prediction and health status assessment mainly encompasses Deep Belief Networks (DBN) (Peng et al., 2019), Long Short-Term Memory networks (LSTM) (Zhang et al., 2018), Gated Recurrent Units (GRU) (Luo et al., 2020), CNN, Graph Neural Networks (GNN) (Kong et al., 2022), and Transfer Learning (TL) (Zhang et al., 2021). These cutting-edge studies are continually advancing the monitoring and lifespan prediction technologies for cable equipment.
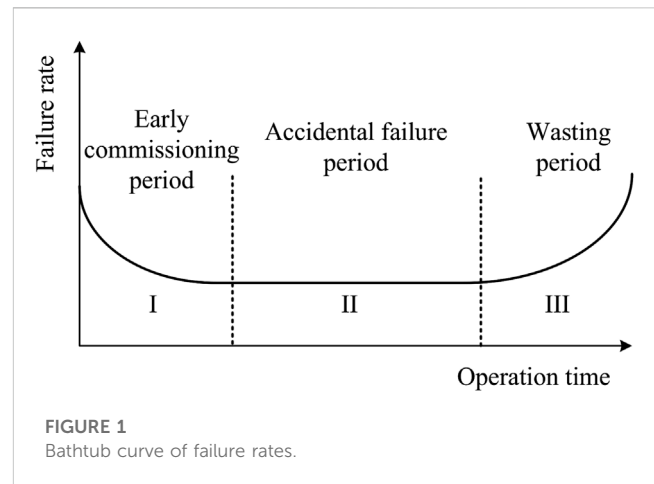

FIGURE 1
Bathtub curve of failure rates.

This paper introduces an innovative approach for assessing and predicting the health status of cables in the context of large-scale electric vehicle (EV) charging loads. The key contributions of this study are summarized as follows:

(1) Development of a cable temperature-current-capacity-life calculation model. This model conducts a comprehensive analysis of both rapid and slow charging scenarios and explores through case studies the impact of different charging scenarios and EV penetration rates on cable temperature. This offers new perspectives and solutions for cable management in EV charging facilities.

(2) Introduction of the concept of a Cable Health Index and the construction of a cable health status assessment framework based on this index. Taking into account various factors that could lead to cable faults, this framework allows for a comprehensive health assessment of cables with different fault rates, significantly enhancing the safety and efficiency of cable usage.

(3) Proposal of a predictive method that combines the FHO Algorithm with a CNN. This method uses the FHO algorithm to optimize the hyperparameters of the BiGRU, enhancing predictive performance. It effectively searches and determines the optimal hyperparameter configuration, enabling precise assessment and prediction of cable health status.

The remainder of the paper is organized as follows: Section 2 constructs the cable model considering EV charging demands and analyzes rapid and slow charging requirements. Section 3 presents a deep learning-based method for predicting the health status of cable equipment. Section 4 offers simulation results and discusses the outcomes of the tests. Finally, Section 5 concludes the study.

2 Cable model considering EV charging demand

The historical data of cables include operational years and routine inspections. As operational years increase, the condition of the cables deteriorates. The lifecycle of a cable follows a "bathtub curve," which can be divided into three phases: the early debugging
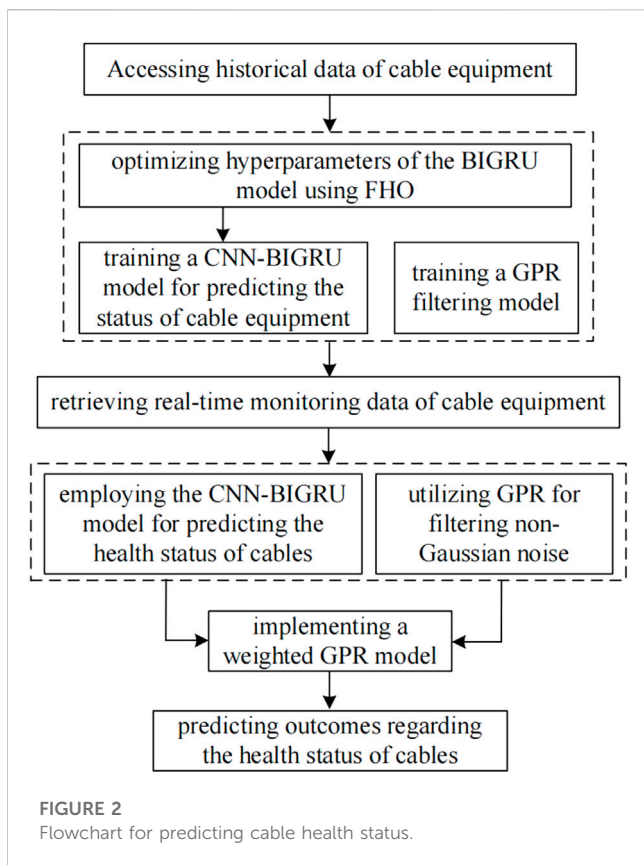
FIGURE 2
Flowchart for predicting cable health status.

period, the random failure period, and the wear-out period, as illustrated in Figure 1.

To quantify the impact of EV charging loads on cables, this paper constructs a cable equipment temperature-current-capacity-life calculation model, considering both rapid and slow EV charging demands.

2.1 Slow charging demand

Considering that the charging mode allows EVs to charge without exceeding the battery capacity and that the constant current process in a complete slow charging cycle is very short, the entire slow charging process is approximated as constant voltage charging. Assuming that the charging current for slow charging is 0.1C (C refers to battery capacity), the charging power Pc of a typical EV falls within the range of 2–3 kW and follows a uniform distribution, with its probability distribution function as (Eq. 1)

$$f_{P_c}(x) = \begin{cases} 1 & x \in [2,3] \\ 0 & \text{otherwise} \end{cases} \qquad (1)$$

The time required for each EV's slow charging is calculated as (Eq. 2)

$$T_c = \frac{SW_{100}}{100P_c} \qquad (2)$$

Considering two types of slow charging modes: dispersed and centralized, this study focuses on dispersed slow charging for both pure electric and hybrid vehicles. Assuming that all slow-charging

EVs finish their last daily trip and return to their parking spots at the time which marks the beginning of charging. Based on a survey of American household vehicles, the start time of charging is also approximated as a normal distribution, with the specific probability density function as (Eq. 3):

$$f_s(x) = \begin{cases} \dfrac{1}{\sigma_s \sqrt{2\pi}} \exp\left[-\dfrac{(x-\mu_s)^2}{2\sigma_s^2}\right] & (\mu_s - 12) < x \le 24 \\[3mm] \dfrac{1}{\sigma_s \sqrt{2\pi}} \exp\left[-\dfrac{(x+24-\mu_s)^2}{2\sigma_s^2}\right] & 0 < x \le (\mu_s - 12) \end{cases} \qquad (3)$$

With the initial scale of EVs in the region, combining the EV driving mileage and charging start time, the remaining battery charge of each vehicle can be calculated.

2.2 Rapid charging demand

In rapid charging mode, the initial phase of EV charging generally involves constant current charging, following an exponential distribution. When the battery is charged to 80% of its rated capacity, the process is as (Eq. 4):

$$P_{fc}(t) = P_N e^{-\frac{P_N}{(0.9-SOC_0)C}t} \qquad (4)$$

For instance, $P_N = 100$ kW, for a battery capacity of 60 kW and a remaining charge of 40%, an EV would require approximately 0.67 h to charge.

The extent of EV charging and battery swapping demand is primarily influenced by user behavior, battery capacity, and the technical level of charging equipment. At a certain stage of development, constrained by the level of technology, battery capacity and the power rating of charging equipment are generally fixed, hence EV charging and swapping demand mainly depends on daily driving mileage.

To obtain the daily load curve of EV charging and swapping, it is first necessary to know the daily driving mileage S of EV users and the electric energy W_{100} consumed per 100 km by the EV. The product of these two factors gives the daily power consumption of the EV. Based on relevant statistical survey data, the daily mileage is approximated to fit a log-normal distribution, with the corresponding probability density function as (Eq. 5):

$$f(d) = \frac{1}{d\sigma_{D,i}\sqrt{2\pi}} \exp\left[-\frac{(\ln d - \mu_{D,i})^2}{2\sigma_{D,i}^2}\right], i = 1, 2, ..., 7 \qquad (5)$$

Compared to the dispersed slow charging mode, the rapid charging mode sees a higher degree of charging demand, mainly affected by the power consumption during various time periods. This paper assumes that the distribution of start times for rapid charging is consistent with the swapping time distribution in the swapping mode. It is also assumed that when pure electric and hybrid EVs undergo rapid charging, the remaining battery charge follows a normal distribution of (0.4, 0.133), leading to a specific probability density function for the remaining battery capacity (Eq. 6).

$$f_K(x) = \frac{1}{\sigma_K \sqrt{2\pi}} \exp\left[-\frac{(x-\mu_K)^2}{2\sigma_K^2}\right] \qquad (6)$$

2.3 Cable temperature calculation model

The introduction of nonlinear loads by AC charging of EVs leads to the generation of harmonics. These harmonic signals affect both voltage and current, encompassing harmonic voltage and current. According to the definition by IEC 61000, these are represented as (Eq. 7) and (Eq. 8):

$$\sigma_{\text{THD}u} = \frac{\sqrt{\sum_{2}^{n} U_n^2}}{U_1} \tag{7}$$

$$\sigma_{\text{THD}i} = \frac{\sqrt{\sum_{2}^{n} I_n^2}}{I_1} \tag{8}$$

As per the IEC 60287 standard, the core temperature θ of a 10 kV three-core cable can be expressed as $\theta = \theta_c + \theta_0$, the values of related parameters can be found in Wang et al. (2019) θ_c can be calculated by (Eq. 9).

$$\theta_c = \sum_{i=1}^{n} I_i^2 R_{\text{AC}}(i) (T_1 + c_i T_2 + c_i (1 + \lambda_2(i)) (T_3 + T_4)) \tag{9}$$

2.4 Cable current carrying capacity calculation model

The harmonic currents generated during the charging process of EVs can cause the total current carrying capacity of the cable to exceed its design value, potentially leading to overload and safety issues. The current carrying capacity of 10 kV three-core cable can be calculated using (Eq. 10)

$$I_{h,\text{rated}} = \sqrt{\Delta \theta_c \Big/ \sum_{i=1}^{n} \frac{I_i^2}{I_1^2} R_{AC}(i) (T_1 + (1 + \lambda_1(i))T_2 + (1 + \lambda_1(i) + \lambda_2(i)) (T_3 + T_4))} \tag{10}$$

2.5 Cable life calculation model

The harmonic currents produced during the EV charging process cause additional heating in the cable, affecting its thermal life. The cable's life per hour is given by (Eq. 11):

$$L_h(t) = 8760 \cdot L_0 e^{-\frac{\Delta w}{k_B T(t)}} \tag{11}$$

The daily life degradation of the cable is expressed as (Eq. 12):

$$L_d = \sum_{t=1}^{24} \frac{1}{L_h(t)} \tag{12}$$

2.6 Failure rate model

Cable fault sample data follow a Weibull distribution with the sought parameters. Such a function can simulate various fault factors by selecting appropriate parameters and can also assess the systemic reliability when the cable fault rate dynamically changes. The mathematical model for cable fault rate is shown as (Eq. 13):

$$\lambda(t) = \frac{\beta}{\eta} \left(\frac{t}{\eta} \right)^{\beta - 1} \tag{13}$$

To account for the difference in cable fault rates before and after maintenance, this paper introduces an age regression factor α, representing the actual change in cable fault rate. The actual service age of the cable is then given by (Eq. 14):

$$T_{\text{real}} = T - \alpha T = (1 - \alpha)T \tag{14}$$

This allows for the determination of the fault rate after the k-th maintenance. As shown in (Eq. 15).

$$\lambda_k(t) = \lambda[t + (1 - \alpha)kT] = \frac{\beta}{\eta} \left[\frac{t + (1 - \alpha)kT}{\eta} \right]^{\beta - 1} \tag{15}$$

3 Deep learning-based method for predicting the health status of cable equipment

To avoid the issues of cable current carrying capacity overload and temperature rise caused by concentrated EV charging, this study proposes a data-driven and weighted Gaussian regression method for predicting the operational state of cable equipment. This approach utilizes CNN and LSTM networks to predict parameters of cable equipment, thereby enhancing the performance of Gaussian Process Regression (GPR), aiming to improve the accuracy of predicting parameters like cable temperature and current carrying capacity.

The proposed FHO-CNN-BIGRU method for predicting the operational state of cable equipment employs the CNN algorithm to mine data relationships and mitigate noise interference. The extracted features are then fed into a BiGRU model optimized by the FHO Algorithm for time series prediction, enhancing the stability of the forecasts. Additionally, this method incorporates a GPR filtering model to smooth the data using Gaussian process regression, thus improving data accuracy and reliability. The cable health status prediction flow chart is shown in Figure 2.

3.1 FHO optimization of BiGRU hyperparameters

The FHO algorithm is a meta-heuristic algorithm that simulates the foraging behavior of fire hawks, considering processes like setting fires, spreading, and capturing prey. Initially, several candidate solutions are determined as the location vectors of the fire hawks and prey, using a random initialization process as per the given formula to identify these vectors' initial positions in the search space. As shown in (Eq. 16) and (Eq. 17).

$$X = \begin{bmatrix} X_1 \\ \vdots \\ X_i \end{bmatrix} = \begin{bmatrix} x_1^1 x_1^2 \cdots x_1^j \\ \vdots \\ x_i^1 x_i^2 \cdots x_i^j \end{bmatrix}, \begin{cases} i = 1, 2, \dots, N \\ j = 1, 2, \dots, D \end{cases} \tag{16}$$

$$x_i^j(0) = x_{i,\min}^j + rand \cdot \left(x_{i,\max}^j - x_{i,\min}^j\right) \qquad (17)$$

The distance between a fire hawk m and prey n is calculated to determine the nearest prey around each fire hawk and define their territories. As shown in (Eq. 18).

$$D_n^m = \sqrt{(x_n - x_m)^2 + (y_n - y_m)^2} \qquad (18)$$

Then, positions are updated: fire hawk m collects burning sticks from the main fire and throws them into a specific area to force the prey to flee. The detailed process of updating positions can be referred to in the cited literature (Azizi et al., 2023).

Based on the solution process of the aforementioned FHO optimization algorithm, the steps to optimize the BiGRU model hyperparameters are as follows:

Step 1: Define the Hyperparameter Search Space. Identify the hyperparameters of the BiGRU model to be optimized and establish a range or a set of possible values for each hyperparameter.

Step 2: Initialize Solution Candidates. Generate initial solution candidates of hyperparameter combinations randomly, in accordance with the defined search space.

Step 3: Evaluate Initial Solution Candidates. Employ cross-validation or other suitable methods to train the model and assess the performance of the initial solution candidates, calculating their fitness values (such as accuracy, loss function values, etc.).

Step 4: Set the Global Optimum. Designate the best solution among the initial candidates as the global optimum.

Step 5: Iterative Optimization. Continuously update the hyperparameter combinations by generating falcons and prey. The distance between falcons and prey is computed, and territories of the falcons are determined. Falcons update their hyperparameter combinations based on their positions, and prey both within and outside the territories also update their combinations. By evaluating the fitness values of the updated hyperparameter combinations and updating the global optimum to the current best solution, the FHO algorithm progressively searches for improved hyperparameter combinations, thereby enhancing the BiGRU model's performance through iterative optimization.

Step 6: Return the Global Optimum. Upon completion of the iterations, the global optimum is returned as the optimized set of hyperparameters for the BiGRU model.

3.2 FHO-CNN-BiGRU prediction model

Step 1: Data Preprocessing. Undertake preparatory processing of the monitoring data for cable equipment, involving data cleansing and normalization among other procedures, to ready the input data.

Step 2: Feature Extraction. Utilize a CNN to extract salient features from the cable equipment monitoring data, capturing key temporal sequence characteristics.

Step 3: Sequence Modeling. Employ a BiGRU to model the extracted time series features, considering both historical and prospective state information.

Step 4: Predictive Output. Utilize the terminal temporal step's BiGRU hidden state as the vector representation of the equipment's health status, and input this into a fully connected layer for the prediction of the health state.

Step 5: Model Optimization. Apply the FHO algorithm to refine hyperparameters such as the convolutional kernel size, GRU's hidden unit count, learning rate, and other factors pertinent to model performance, thereby enhancing the accuracy of health status prediction.

Step 6: Model Evaluation. Assess the model's performance using appropriate metrics (like accuracy, recall, F1 score, etc.), comparing it against the actual health states of the equipment.

Step 7: Health Status Prediction. Utilize the optimized FHO-CNN-BiGRU model to predict the health status of cable equipment based on new monitoring data, thus obtaining prognostications regarding the health state of the cable apparatus.

3.3 Construction of gaussian process regression model

Combining the FHO-CNN-BiGRU prediction model, the GPR model is utilized for its superiority in handling nonlinear problems to obtain nonlinear mappings between measurements and state quantities. The integration of FHO-CNN-BiGRU and GPR algorithms allows for weighting the predicted values from FHO-CNN-BiGRU and the state estimates from GPR, leading to more accurate predictions of the cable equipment's state.

The Gaussian Regression model maps input features to a high-dimensional space through a set of basis functions, denoted as $\psi(\cdot)$, thereby facilitating the discovery of linear relationships among data in this elevated dimensional space. By representing the measured quantities Z, with these basis functions $\psi(\cdot)$, one can derive the probability associated with new data.

The GPR uses confidence judgment to estimate results, which can mitigate noise interference, thereby improving the accuracy of the estimates. Offline training is first conducted based on the nonlinear relationship between historical measurement and state data of cable equipment, followed by state prediction using the trained model based on new measurement data.

3.4 Method for assessing the health status of cable equipment

Aging and deterioration are phenomena that span the entire lifecycle of equipment. Cables, especially those operating in
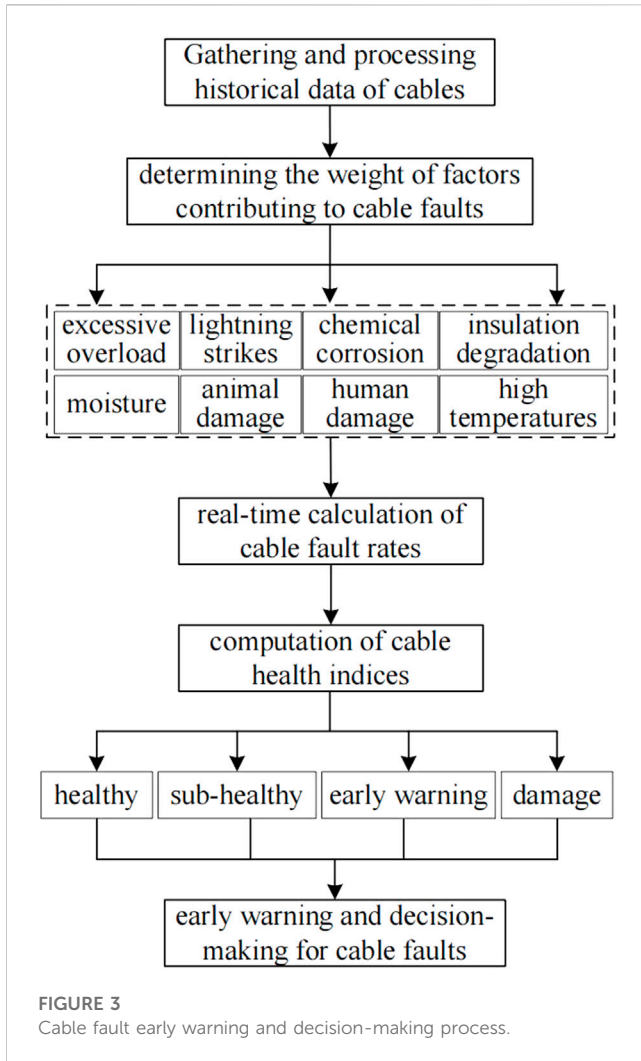
FIGURE 3
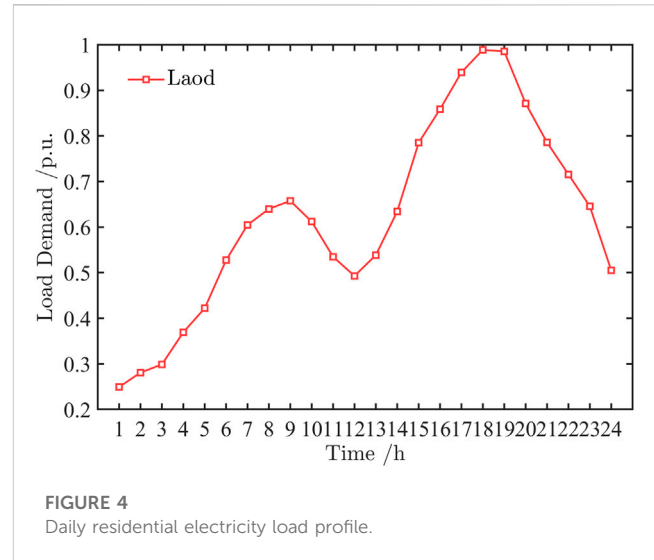Cable fault early warning and decision-making process.

FIGURE 4
Daily residential electricity load profile.
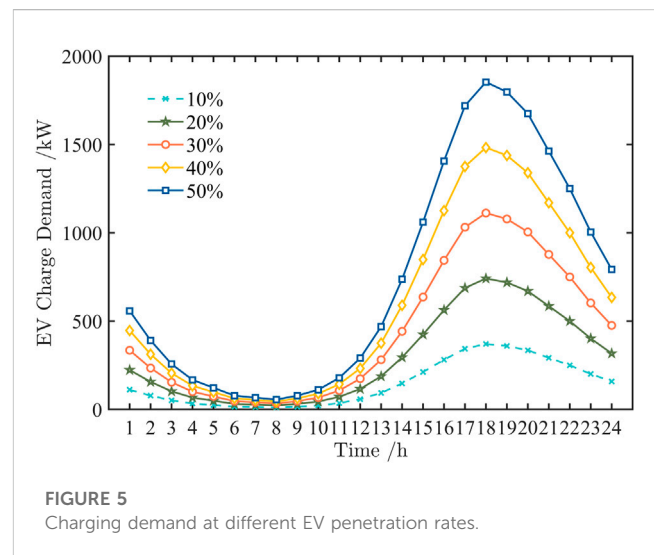
FIGURE 5
Charging demand at different EV penetration rates.

humid environments for extended periods, are prone to water tree aging. The operational state of the cable, maintenance strategies, construction quality, and operating environment significantly impact cable deterioration. Maintenance can enhance the performance of components and extend the equipment's life to a certain extent, but it cannot restore the equipment to its original healthy state, as the rate of deterioration remains unchanged. Assessing the health status is an effective way to monitor the condition of cable equipment. Based on the cable status prediction results, this paper introduces the concept of a Cable Health Index and constructs a cable health status assessment framework based on this index. The cable health status assessment process, as illustrated in Figure 3, involves the following detailed steps:

Step 1: Data Collection and Processing. Utilize distributed fiber optic sensors to collect relevant data of the cable, including its lifespan, insulation thermal resistance, and other parameters. Combine these with predicted parameters like current carrying capacity, temperature, and lifespan to construct a health status assessment dataset. Analyze and process the collected data,

employing methods like Principal Component Analysis to remove redundant features and repair missing data.

Step 2: Determination of Cable Fault Factor Weights. Considering the operational conditions of the cable, use the Analytic Hierarchy Process to calculate the weights of factors that could potentially cause cable faults, obtaining the weight w_i for the ith type of fault factor. Factors include heavy overload, lightning strikes, high temperatures, humidity, chemical corrosion, human-induced damage, animal damage, and insulation aging.

Step 3: Calculation of Cable Fault Rate. Calculate the cable fault rate $\lambda(t)$ and the fault rate λ_k after kth maintenance using the designated (Eq. 19). Modify the fault rate based on the cable's service age using the appropriate (Eq. 20) to obtain the real-time fault rate.

FIGURE 6
Cable temperature variations under different EV penetration rates.

FIGURE 7
Temperature impacts in slow charging scenarios at different EV penetration rates.
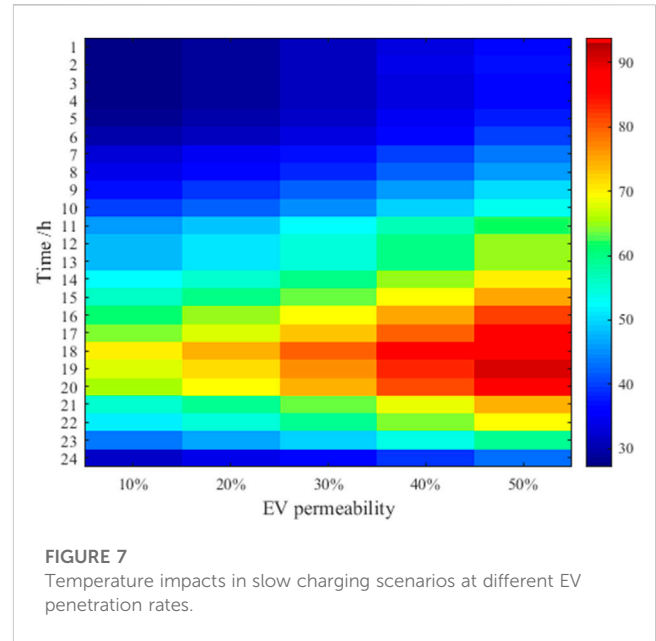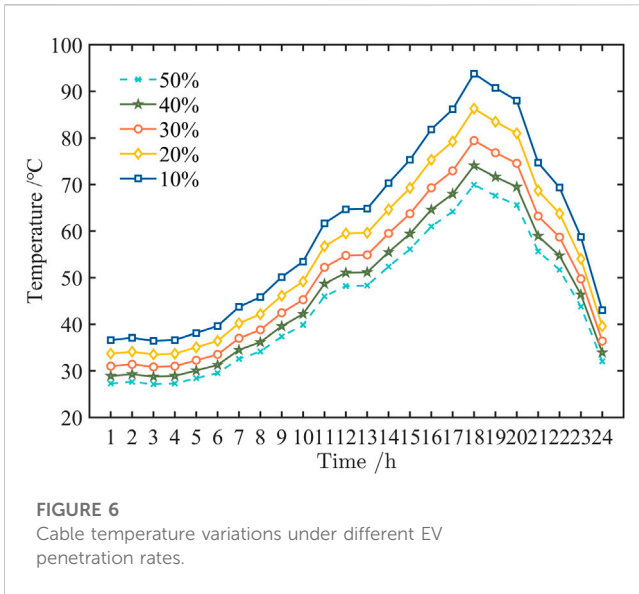
$$\lambda(t) = \begin{cases} 0.0198 & t \le 20 \\ \dfrac{6.849}{35.536} \times \left(\dfrac{t}{35.536}\right)^{5.849} & t > 20 \end{cases} \tag{19}$$

$$\lambda^{\star} = w_i \cdot \lambda_k \tag{20}$$

Step 4: Calculation of Cable Health Index. Utilize the real-time fault rate to calculate the cable's real-time health index $H^{\star}$. As shown in (Eq. 21).

$$H^{\star} = \frac{1}{\xi}\ln\left(\frac{\lambda^{\star}}{K}\right) \tag{21}$$

Step 5: Assessment of Cable Health Status. Based on the calculated real-time health index, assess the health status of the cable. Categorize the cable into different health statuses, including healthy, sub-healthy, early warning, and damaged, according to predefined standards and thresholds.

Step 6: Early Warning and Decision-Making. Set warning thresholds based on the real-time fault rate and health index. When the fault rate exceeds the threshold or the health index declines, the system can issue an alert, prompting maintenance

personnel to take appropriate actions such as repair, replacement, or upgrade of the cable.

4 Case analysis

This paper focuses on a case study of a community with 2000 private EVs. For simplicity in the simulation, it is assumed that EVs charge at a constant power, with a battery capacity of 70 kWh. The study considers AC slow charging and DC fast charging, setting the ratio of fast to slow charging at 3:7. According to the standard charging modes defined in IEC61851-1, a 6.6 kW AC charging station for electric cars has a current of 32A, and a 35 kW DC charging station has a current of 160A. The temperature limit of XLPE cables is set at 90°C. Due to higher losses in AC cables under the same load conditions compared to DC cables, the temperature changes caused by fast charging are not considered initially. Figure 4 shows the typical daily load curve without considering EV charging, and Figure 5 presents the charging demand curves at different EV penetration rates.

TABLE 1 Maximum cable temperatures at different EV penetration rates in various scenarios.

EV penetration rate	Temperature (°C)		
	Considering harmonics	Disregarding harmonics	Disregarding fast charging
0	63.56	63.56	63.56
10%	67.96	64.85	69.92
20%	71.23	67.55	74.05
30%	76.80	71.61	79.43
40%	83.58	79.56	86.30
50%	91.67	90.03	93.82
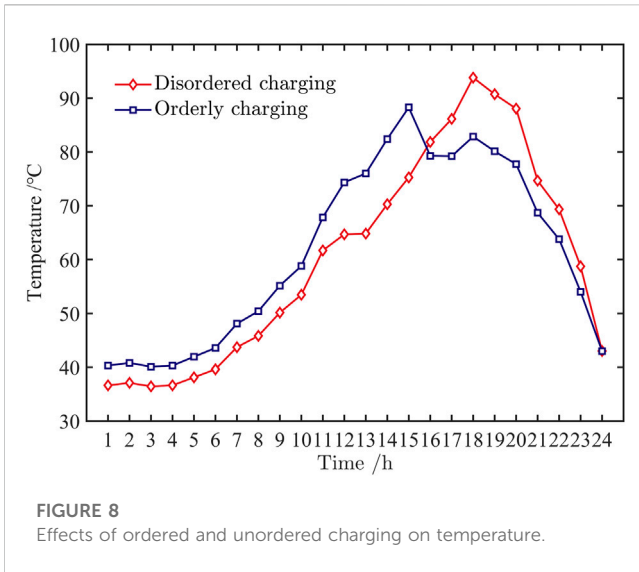
FIGURE 8
Effects of ordered and unordered charging on temperature.

TABLE 2 Health grade classification.

Health index	Health level	Health status
100 ≥ H ≥ 75	S1	Health
75 ≥ H ≥ 50	S2	Sub-health
50 ≥ H ≥ 20	S3	Early warning
20 ≥ H ≥ 0	S4	Damage

FIGURE 9
Fitted curve of cable failure rates.

4.1 Impact of EV charging demand on cables

To assess the impact of different scales of EV integration on cable temperature rise, we analyzed cable temperatures under various charging demands, setting EV penetration rates at 0%, 10%, 20%, 30%, 40%, and 50%. The simulation tested the cable temperature variations in each scenario, as shown in Figure 6; Table 1.

From Figure 6, it is evident that with the increase in the number of EVs, the rising charging demand leads to a continuous increase in cable temperature. Especially when the EV penetration rate reaches half of the total number of private cars in the community, the cable temperature exceeds the permissible limit. At peak demand times, the cable temperature reaches 91.67°C, exceeding the 90°C limit even without considering the impact of harmonics. Therefore, reducing harmonics and improving cable thermal management are crucial for the reliable operation of cables and the entire distribution system. Implementing rational orderly charging strategies or incentivizing users to charge during off-peak hours through time-of-use tariffs could mitigate the risk of cable current exceeding limits due to the cumulative demand of charging and base electrical loads.

4.2 Impact of EV charging strategies on cables

To verify the impact of different charging strategies on cable life, the temperature variations under slow charging demands at different EV penetration rates are shown in Figure 7. Additionally, considering the peak and off-peak periods as defined in (Sun et al., 2019), Figure 8 shows the temperature variation curves for two scenarios at a 50% penetration rate under time-of-use charging.

From the figures, it is seen that in uncoordinated charging, all EV users start charging immediately upon returning home, with charging concentrated between 6 p.m. and 2 a.m. the next day. At 6 p.m., the cable temperature reaches 91.67°C due to the peak in total electricity demand from both charging and base loads. Under the influence of time-of-use tariffs, EV users tend to choose lower-priced periods for charging, mostly during the peak hours of solar power generation. Although the surge in
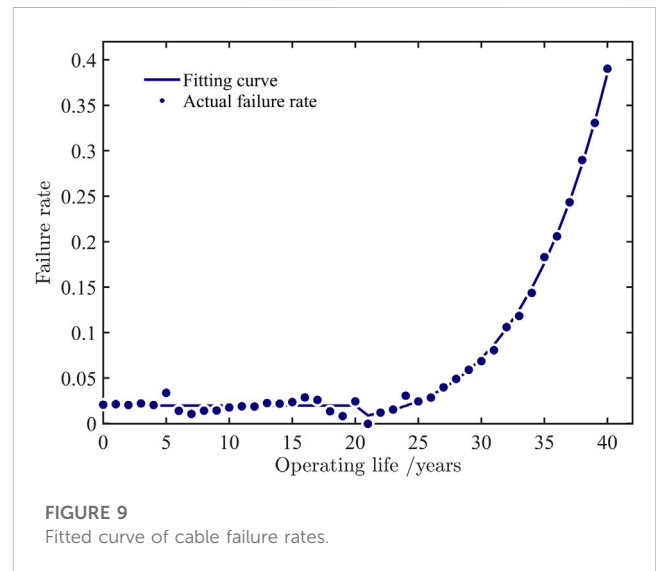
charging demand increases the cable temperature, it effectively avoids the temperature rise caused by "peak upon peak" by occurring during the low-demand period of the grid. The cable temperature remains at 88.28°C, not exceeding its maximum tolerance, thereby reducing the fluctuation range of cable temperature. This strategy not only avoids impact on the cable but also enhances the utilization of solar power in the grid.

4.3 Cable health status assessment and prediction

An analysis is conducted on the operational status of cables under the two charging scenarios mentioned above, and a health status assessment is performed using the health index. The criteria for classifying health levels are shown in Table 2, and the future health status of the cables is predicted using the model proposed in this paper.

As indicated in Table 2, S1 represents equipment that meets all performance standards, with good foundational conditions, intact technical performance, and stable operational conditions, capable of withstanding external environmental risks. S2 denotes equipment with intact functionality and performance, though slightly below the healthy state, still meeting standard operational requirements. S3 indicates equipment in basically good condition, capable of performing specified functions, but with some performance degradation, having a minor overall impact and needing maintenance. S4 signifies equipment with severe technical performance deficiencies, unable to meet operational standards, and posing a threat to system safety and stability, urgently requiring replacement.

TABLE 3 Weighting of fault factors.

Failure factors	Overload	Heavy rain	Lightning strike	High temperature	Others
Weight	0.212	0.356	0.093	0.098	0.241

TABLE 4 Cable failure rates and health information.

Cable	Failure rate	HI	HS	Future HI	Future HS
1	0.020	74.150	S2	67.094	S2
2	0.010	80.090	S1	72.468	S2
3	0.008	81.816	S1	74.030	S2
4	0.004	87.738	S1	79.388	S1
5	0.007	83.380	S1	75.445	S1
6	0.019	74.740	S2	67.628	S2
7	0.004	87.738	S1	79.388	S1
8	0.017	75.309	S2	68.142	S2
9	0.013	77.623	S2	70.236	S2
10	0.007	83.380	S1	75.445	S1

TABLE 5 Comparison of prediction methods.

Method	Accuracy rate (%)			
	S1	S2	S34	Comprehensive
BPNN	76.1	85.7	73.6	79.4
SVM	84.1	87.2	83.8	85.3
Proposed method	92.5	93.6	90.3	92.5

Figure 9 shows an increase in the fault rate of cables over time. Considering the climate environment of the Xiong'an New Area, 100 cables are selected, and the weights of various fault factors are calculated using the Analytic Hierarchy Process, as shown in Table 3.

The cable fault rate and health index are calculated based on the weights of the fault factors and used as initial parameters to predict future changes in the cable's health status. Table 4 presents the fault rates and health information of 10 selected cables and predicts their future health status.

4.4 Comparison of prediction method efficacy

To validate the superiority of the method proposed in this study, its prediction results were compared with those of the Back Propagation Neural Network (BPNN) and Support Vector Machine (SVM) models, as shown in Table 5. S1 and S2 respectively correlate to the health grades outlined in Table 2. The amalgamation of S3 and S4, denoted as S34, indicates that the cable is in a state of malfunction or pre-alert.

The analysis of the provided data in Table 5 reveals a clear superiority of the proposed method in accuracy rates across all categories. It surpasses both BPNN and SVM, achieving 92.5% in

S1, 93.6% in S2, and 90.3% in the combined S34 category, with a comprehensive accuracy of 92.5%. This consistently higher performance across all metrics establishes the "Proposed Method" as the most effective and accurate among the methods evaluated.

5 Conclusion

In this paper, we proposed a method for assessing and predicting the health status of cables under the load of large-scale EV charging. Through detailed case analysis, the following conclusions were drawn:

(1) The increase in EV charging demand poses a risk of exceeding cable temperature limits, particularly under the influence of harmonics in AC slow charging scenarios. Addressing this involves both reducing harmonic interference and enhancing cable thermal management, which are essential for ensuring the reliability of the cable system and the overall distribution network.

(2) Cables experience more severe operational challenges and increased risk, especially with prolonged use of AC slow charging by EVs. Implementing time-of-use tariffs to encourage orderly charging can mitigate issues like cable current overload from cumulative charging and base load demands. Additionally, at a 50% EV penetration rate, uncoordinated charging can lead to cable overloading, while time-of-use tariffs can help regulate charging demand distribution, thus reducing peak-to-valley differences and lowering cable temperatures during high grid load periods.

(3) The method proposed in this paper for assessing and predicting cable health status effectively evaluates the operational state of cables and issues timely warnings. It accurately predicts future changes in cable health, providing essential support for grid dispatchers to arrange maintenance and operation plans, thereby enhancing the reliability of the distribution system.

Future research will aim to enhance predictive models and thermal management, facilitating efficient integration of EVs into the electrical grid.

Data availability statement

The original contributions presented in the study are included in the article/supplementary material, further inquiries can be directed to the corresponding author.

Author contributions

HL: Conceptualization, Writing–original draft. LR: Data curation, Writing–review and editing. TB: Software, Writing–review and editing.

ZK: Methodology, Writing–review and editing. JB: Validation, Writing–review and editing. XL: Resources, Writing–review and editing.

Conflict of interest

Authors HL, LR, TB, ZK, JB, XL were employed by State Grid XiongAn New Area Electric Power Supply Company.

The authors declare that this study received funding from Hebei Electric Power Company of State Grid. The funder had the following involvement in the study: design, collection, analysis, interpretation of data, the writing of this article and the decision to submit it for publication.

Publisher's note

All claims expressed in this article are solely those of the authors and do not necessarily represent those of their affiliated organizations, or those of the publisher, the editors and the reviewers. Any product that may be evaluated in this article, or claim that may be made by its manufacturer, is not guaranteed or endorsed by the publisher.

References

Ahmad, T., Madonski, R., Zhang, D., Huang, C., and Mujeeb, A. (2022). Data-driven probabilistic machine learning in sustainable smart energy/smart energy systems: key developments, challenges, and future research opportunities in the context of smart grid paradigm. *Renew. Sustain. Energy Rev.* 160, 112128. doi:10.1016/j.rser.2022.112128

Azizi, M., Talatahari, S., and Gandomi, A. H. (2023). Fire Hawk Optimizer: a novel metaheuristic algorithm. *Artif. Intell. Rev.* 56, 287–363. doi:10.1007/s10462-022-10173-w

Carvalho, T. P., Soares, F. A. A. M. N., Vita, R., Francisco, R. da P., Basto, J. P., and Alcalá, S. G. S. (2019). A systematic literature review of machine learning methods applied to predictive maintenance. *Comput. Ind. Eng.* 137, 106024. doi:10.1016/j.cie.2019.106024

Dinmohammadi, F., Flynn, D., Bailey, C., Pecht, M., Yin, C., Rajaguru, P., et al. (2019). Predicting damage and life expectancy of subsea power cables in offshore renewable energy applications. *IEEE Access* 7, 54658–54669. doi:10.1109/ACCESS.2019.2911260

Gan, L., Wu, H., and Zhong, Z. (2022). Fatigue life prediction considering mean stress effect based on random forests and kernel extreme learning machine. *Int. J. Fatigue* 158, 106761. doi:10.1016/j.ijfatigue.2022.106761

Gupta, R. S., Tyagi, A., and Anand, S. (2021). Optimal allocation of electric vehicles charging infrastructure, policies and future trends. *J. Energy Storage* 43, 103291. doi:10.1016/j.est.2021.103291

Han, T., Pang, J., and Tan, A. C. C. (2021). Remaining useful life prediction of bearing based on stacked autoencoder and recurrent neural network. *J. Manuf. Syst.* 61, 576–591. doi:10.1016/j.jmsy.2021.10.011

Hossain, E., Roy, S., Mohammad, N., Nawar, N., and Dipta, D. R. (2021). Metrics and enhancement strategies for grid resilience and reliability during natural disasters. *Appl. Energy* 290, 116709. doi:10.1016/j.apenergy.2021.116709

Kong, Z., Jin, X., Xu, Z., and Zhang, B. (2022). Spatio-temporal fusion attention: a novel approach for remaining useful life prediction based on Graph neural network. *IEEE Trans. Instrum. Meas.* 71, 1–12. doi:10.1109/TIM.2022.3184352

Li, S., and Li, J. (2017). Condition monitoring and diagnosis of power equipment: review and prospective. *High. Volt.* 2, 82–91. doi:10.1049/hve.2017.0026

Li, S., Li, J., Zhang, X., Gockenbach, E., Wasserberg, V., and Borsi, H. (2007). Estimation of the lifetime of the electrical components in distribution networks. *IEEE Trans. Power Del* 22, 515–522. doi:10.1109/TPWRD.2006.876661

Liao, L., and Kottig, F. (2014). Review of hybrid prognostics approaches for remaining useful life prediction of engineered systems, and an application to battery life prediction. *IEEE Trans. Rel.* 63, 191–207. doi:10.1109/TR.2014.2299152

Luo, Q., Chang, Y., Chen, J., Jing, H., Lv, H., and Pan, T. (2020). Multiple degradation mode analysis via gated recurrent unit mode recognizer and life predictors for complex equipment. *Comput. Ind.* 123, 103332. doi:10.1016/j.compind.2020.103332

Montanari, G. C., Hebner, R., Morshuis, P., and Seri, P. (2019). An approach to insulation condition monitoring and life assessment in emerging electrical environments. *IEEE Trans. Power Del.* 34, 1357–1364. doi:10.1109/TPWRD.2019.2897905

Nemati, M., Sant'Anna, A., Nowaczyk, S., Jürgensen, J. H., and Hilber, P. (2019). Reliability evaluation of power cables considering the restoration characteristic. *Int. J. Electr. Power Energy Syst.* 105, 622–631. doi:10.1016/j.ijepes.2018.08.047

Peng, K., Jiao, R., Dong, J., and Pi, Y. (2019). A deep belief network based health indicator construction and remaining useful life prediction using improved particle filter. *Neurocomputing* 361, 19–28. doi:10.1016/j.neucom.2019.07.075

Rajendran, G., Vaithilingam, C. A., Misron, N., Naidu, K., and Ahmed, M. R. (2021). A comprehensive review on system architecture and international standards for electric vehicle charging stations. *J. Energy Storage* 42, 103099. doi:10.1016/j.est.2021.103099

Sun, Y., Yue, H., Zhang, J., and Booth, C. (2019). Minimization of residential energy cost considering energy storage system and EV with driving usage probabilities. *IEEE Trans. Sustain. Energy* 10, 1752–1763. doi:10.1109/TSTE.2018.2870561

Wang, H., Zhou, W., Qian, K., and Meng, S. (2019). Modelling of ampacity and temperature of MV cables in presence of harmonic currents due to EVs charging in electrical distribution networks. *Int. J. Electr. Power Energy Syst.* 112, 127–136. doi:10.1016/j.ijepes.2019.04.027

Yan, M., Wang, X., Wang, B., Chang, M., and Muhammad, I. (2020). Bearing remaining useful life prediction using support vector machine and hybrid degradation tracking model. *ISA Trans.* 98, 471–482. doi:10.1016/j.isatra.2019.08.058

Yu, H., Niu, S., Shang, Y., Shao, Z., Jia, Y., and Jian, L. (2022). Electric vehicles integration and vehicle-to-grid operation in active distribution grids: a comprehensive review on power architectures, grid connection standards and typical applications. *Renew. Sustain. Energy Rev.* 168, 112812. doi:10.1016/j.rser.2022.112812

Zhang, J., Wang, P., Yan, R., and Gao, R. X. (2018). Long short-term memory for machine remaining life prediction. *J. Manuf. Syst.* 48, 78–86. doi:10.1016/j.jmsy.2018.05.011

Zhang, W., Li, X., Ma, H., Luo, Z., and Li, X. (2021). Transfer learning using deep representation regularization in remaining useful life prediction across operating conditions. *Reliab. Eng. Syst. Saf.* 211, 107556. doi:10.1016/j.ress.2021.107556

Nomenclature

Parameters

T_c	Charging duration
S	Daily driving mileage of the EV
W_{100}	Power consumption per 100 km, in kWh/(100 km)
μ_s, σ_s	Mean and variance
C	Rated battery capacity
SOC_0	Initial state of charge
R_{AC}	AC resistance
T_1	Thermal resistance of the insulation layer
T_2	Thermal resistance from the shielding layer to the armor layer
T_3	Thermal resistance of the armor layer and the outer sheath
T_4	External thermal resistance
c_i	Number of cable cores
θ_0	Ambient temperature
k_B	Boltzmann constant
L_0	Designed lifespan of the cable
Δw	Activation energy
β	Shape parameter
η	Scale parameter
$x_{i,max}^j$	Upper bound
$x_{i,min}^j$	Lower bound
D	Dimension
ξ	Curvature coefficients
K	Proportionality coefficients

Variables

P_N	Rapid charging power
I_1, I_n	Effective values of the fundamental and nth harmonic currents, respectively
U_1, U_n	Effective values of the fundamental and nth harmonic voltages, respectively
h	Order of the higher harmonics
λ_1	Ratio of the shield layer loss to the conductor loss
λ_2	Proportion of loss attributed to the armor layer
θ_c	Temperature rise of the cable
$L_h(t)$	Cable's life at time t
$T(t)$	Cable's temperature at time t hours
X_i	ith candidate solution
N	Total number of candidate solutions
x_i^j	jth decision variable representing the ith candidate solution
H^*	Cable's real-time health index

$\lambda(t)$	Cable fault rate
λ_k	Fault rate after kth maintenance
$\psi(\cdot)$	Basis functions
Z	Measured quantities